What is the magma storage depth under Osorno Volcano (41°S, CSVZ, Chile)?

Tonin Bechon[a,*], Jacqueline Vander Auwera[a], Olivier Namur[b], Paul Fugmann[a], Olivier Bolle[a], and Luis Lara[c]

[a]Department of Geology, University of Liège, Belgium (*Contact: tonin.bechon@uliege.be) — [b]Department of Earth and Environmental Sciences, University of Leuven, Belgium — [c]SERNAGEOMIN, Chile

Introduction :

The depth at which magma chamber processes take place below magmatic arcs and the parameters controlling them are highly debated. These questions are fundamental for our understanding of the global magma differentiation as well as the formation of the continental crust at convergent margins (Rudnick and Gao, 2003), but also for evaluating the risks associated with volcanic eruptions.

In the Central Southern Volcanic Zone (Central-SVZ) of the Chilean Andes, a thin continental crust (30-40 km) and the occurrence of a major fault zone (Linquiñe-Ofqui) likely favor rapid magma ascent. This segment of the arc is as a consequence one of the most active in Chile with several recent eruptions (e.g. Llaima 2009, Cordon Caulle 2011, Calbuco 2015, Villarrica 2015 & 2019). The Central-SVZ is characterized by dominant mafic lavas (basalts, basaltic andesites), few rhyodacitic lavas and a noticeable compositional (Daly) gap in the intermediate compositions (andesites). Noteworthy, amphibole is usually absent, except in a few volcanoes (e.g. Calbuco) or only occurs as microliths in enclaves, which suggests rather low water contents. These observations contrast sharply with the Northern-SVZ where andesitic lavas are dominant and hydrous phases common.

We focused our research on the eruptive products of Osorno volcano (41°S, CSVZ) located between two volcanoes (Calbuco and Cordon Caulle) which recently showed very explosive eruptions and partly overlies an older Pleistocene eroded volcanic edifice (La Picada). A large series of samples were collected in four units spanning 200 kyr. They define a differentiation trend ranging from tholeiitic basalts to calk-alkaline dacites with a Daly Gap between 58 wt. % and 63 wt. % SiO_2. Plagioclase and olivine are dominant before the gap while plagioclase, clino- and orthopyroxene dominate afterwards.

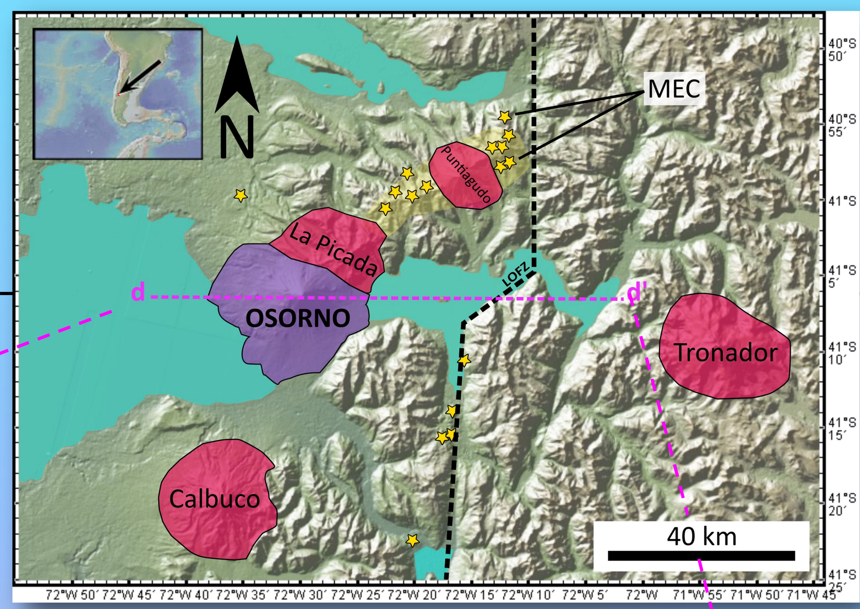

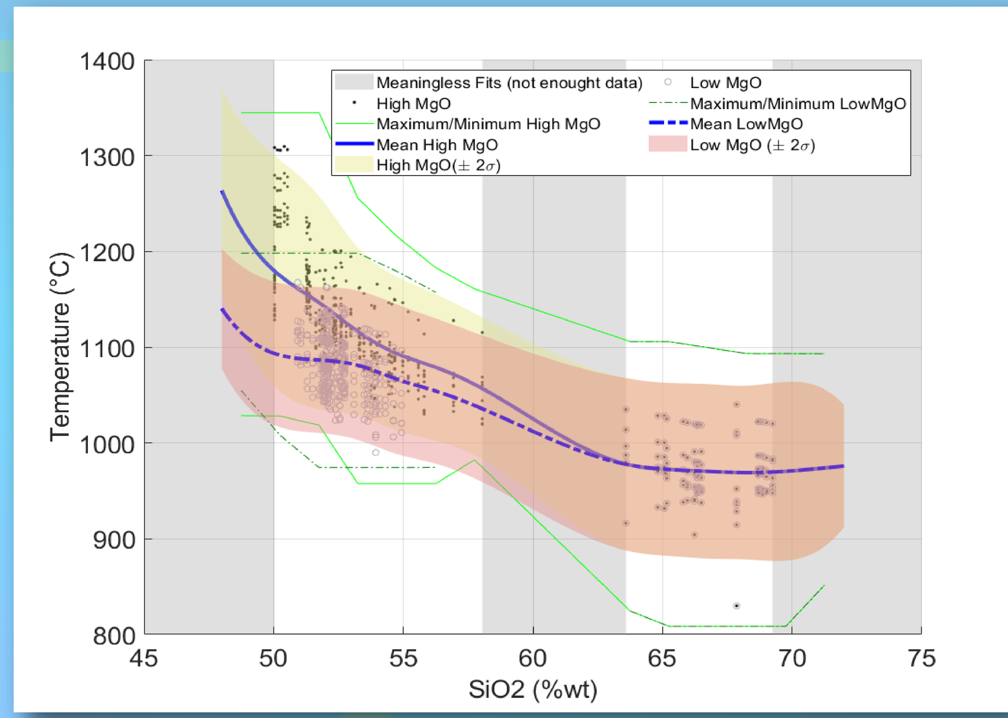

I. Temperature ←

Temperature was calculated using several liq, Ol-Liq, Cpx-Liq, Opx-Liq, Chr-Ol, Apatite thermometers (Putirka, 2008; Wan et al, 2008; Coogan et al, 2014; Harrison and Watson, 1984). As two slightly different trends appeared in the MgOvsSiO2 diagram, data were split between a high- and a low-MgO trend because most of the thermometers may be sensitive to MgO content. When needed, assumptions on pressure (3 ±2 kbar) and H_2O content (2.5 ±2.5 wt%) were made. Displayed points represent respectively 3kbar and 2.5 wt% H_2O. See Figure for results.

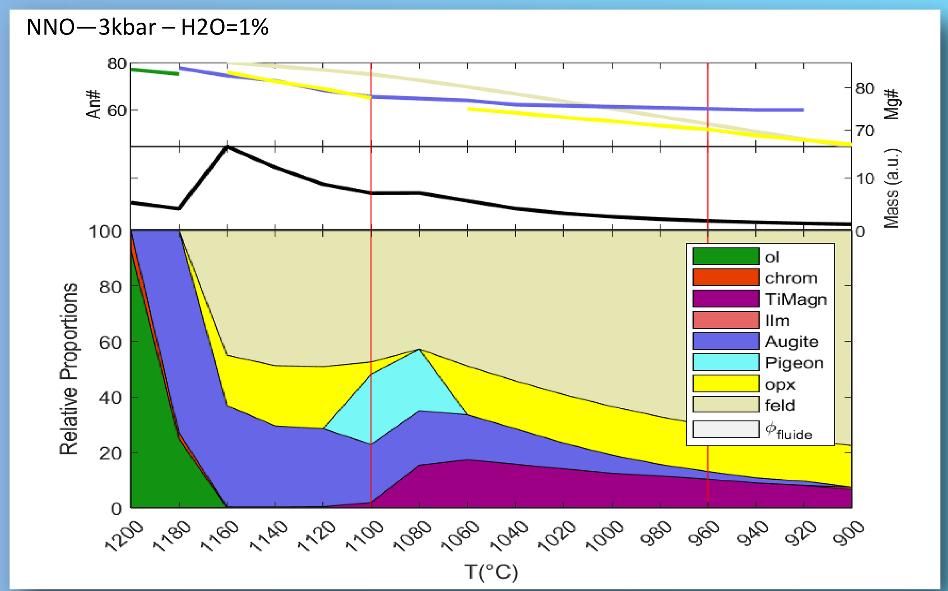

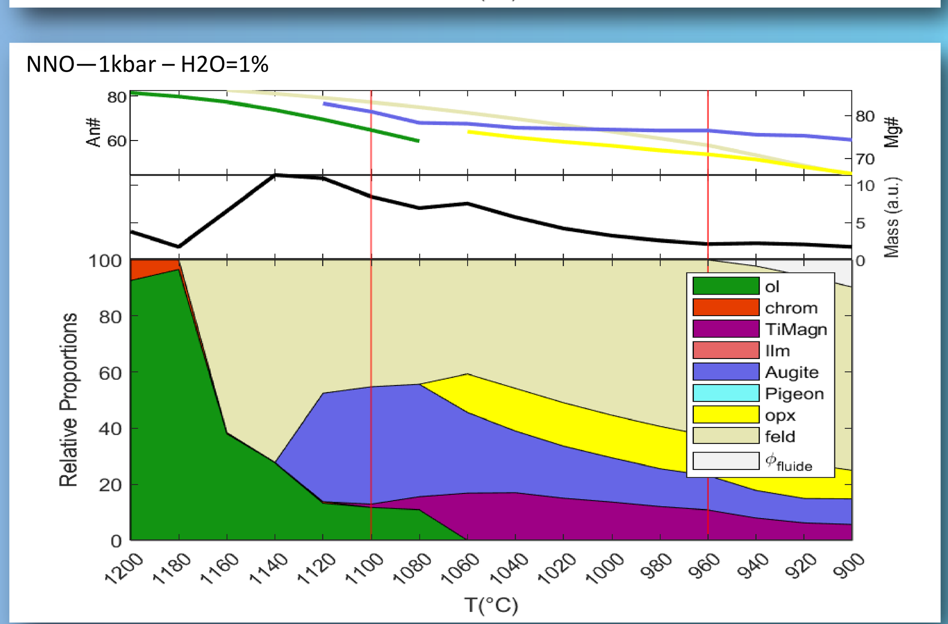

A. Hypersthene and augite dominated dacite (aphyric) →

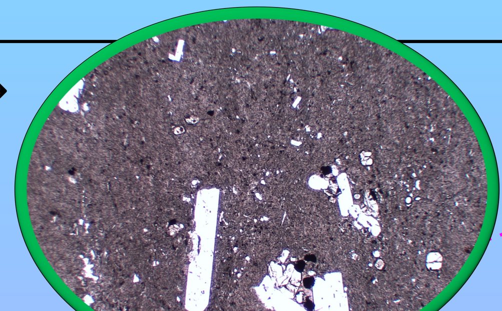

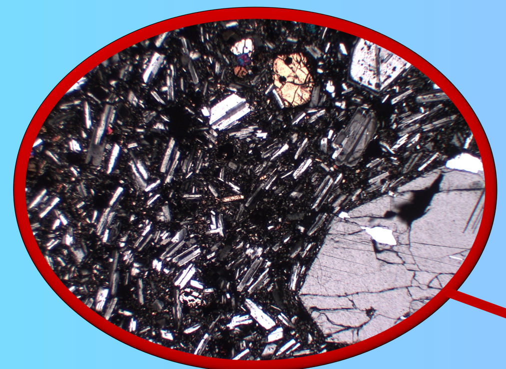

B. Plagioclase and olivine dominated Basaltic-Andesite (porphyric) ↑

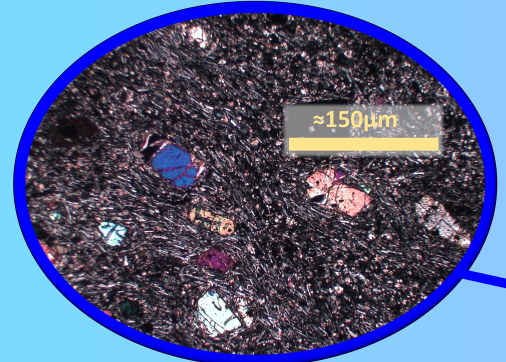

C. Olivine dominated Basalt (aphyric) ↑

(the three images from thin sections are at the same scale)

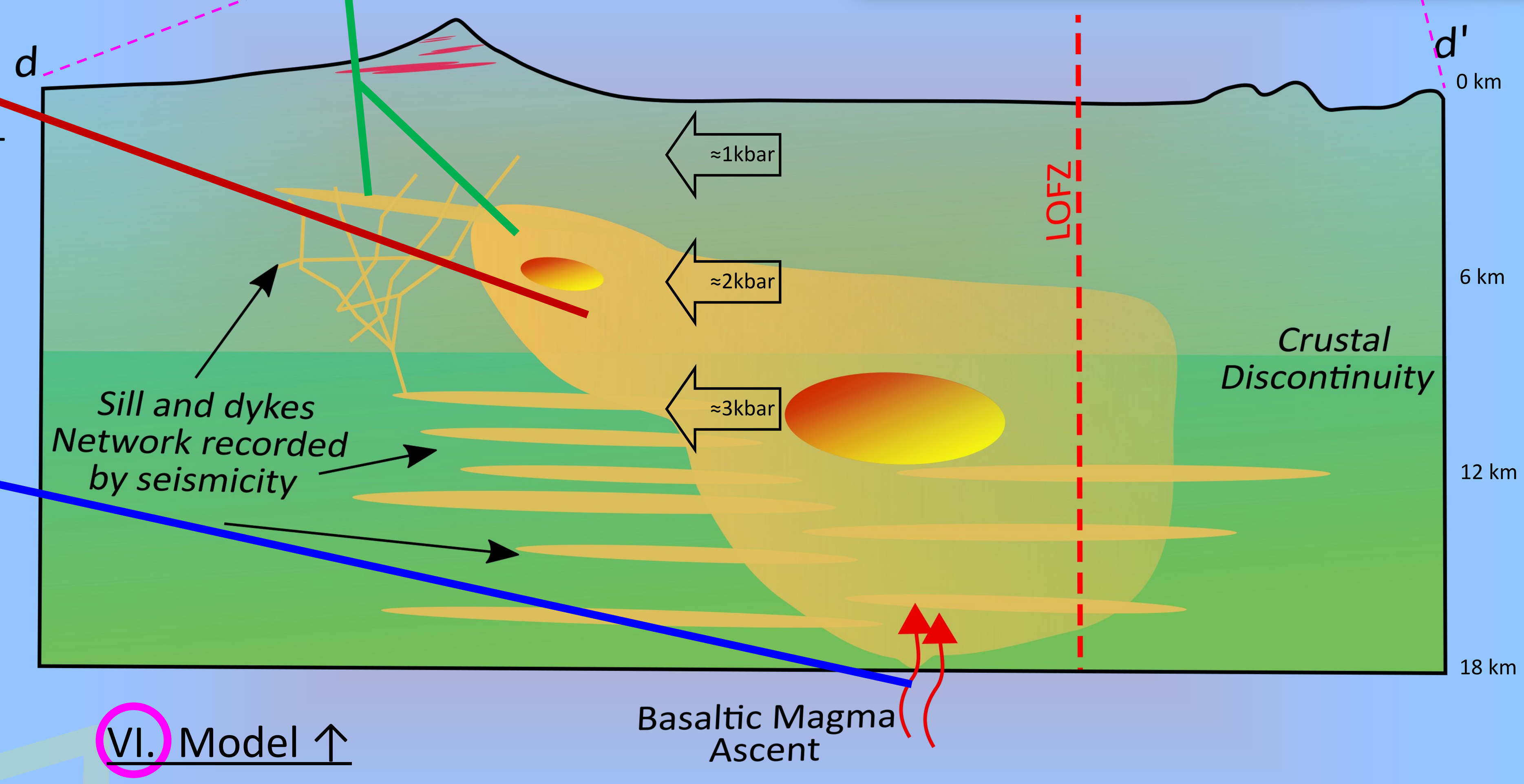

II. Pressure →

Cpx-Liq equilibrium, previously calculated temperatures and same H_2O assumption were used to calculate pressure (Putirka, 2008; Neave et Putirka, 2017). See figure for details. Note that in the absence of Cpx in some thin sections, pressures for mafic lavas were not calculated. The uncertainty is also large.

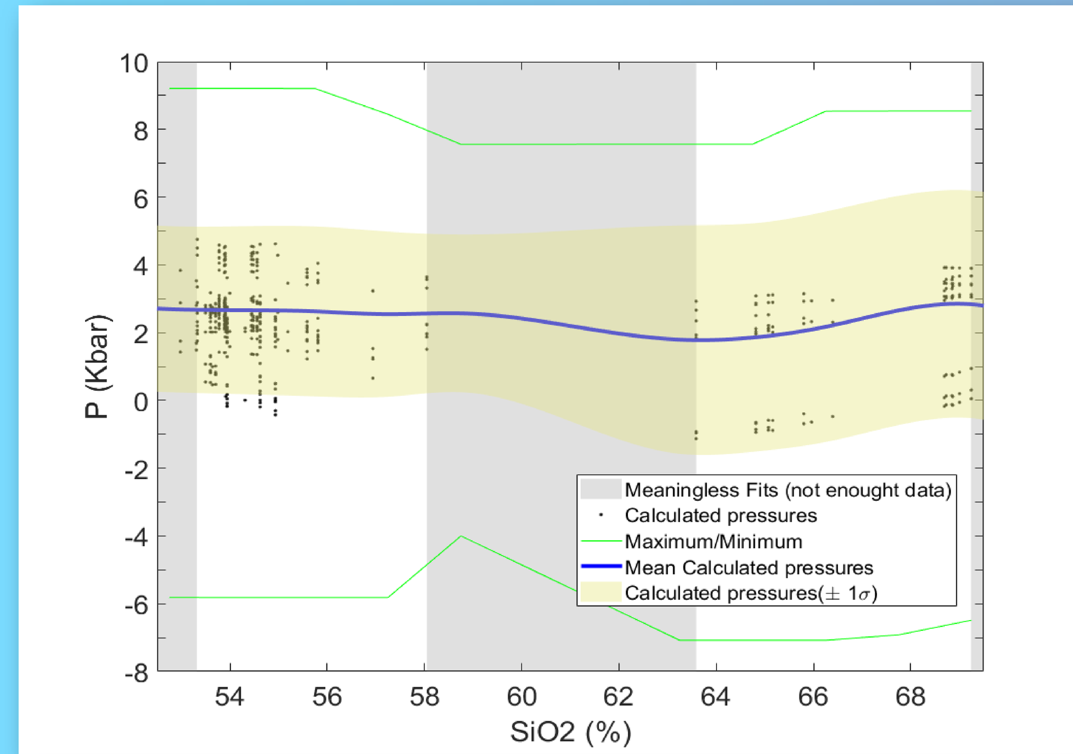

IV. MELTS simulations ↑

Rhyolite-Melts simulations were used to fractionate a mafic basalt at low-pressure (≤4kbar) considering isobaric conditions at NNO. Petrology of our samples is best reproduced at low pressure (1-2kbar) with water initial content in the range 1-2wt%. Each diagram is split into three parts: (1) indications of the chemistry for different phases (Ol, Plag, Cpx, Opx ; the color code is consistent with the caption). (2) indications of the crystallized mass peak during differentiation. (3) Relative proportions of each phase in weight%. Each part is function of the temperature steps used for the simulation. Red vertical lines represent an estimation of the observed Daly gap limits.

VI. Model ↑

The figure above, after Diaz et al. (2020), is a model of the magma chamber under Osorno that was imaged thanks to a geophysical approach. We added a network of sills and dykes according to our interpretation of the seismicity below the volcano (Part V). We understand the system dynamics as follows : (1) input of an undifferentiated basaltic magma from the MOHO (image C, Part III) in the reservoir at low pressure (Part II and III). Here the magma may stagnate, cool and evolve through fractional crystallization (Image B, Part I and IV). It becomes an immobile magmatic mush after a sudden increase of crystallinity between 1100-1000°C. At this point, the only magma that can reach the surface is a dacitic one (= the mush interstitial liquid, image A) or gas and fluids. The dacitic magma being highly viscous, we speculate that external parameters such as the arrival of a new batch of magma reheating the mush or the release of tectonic stresses may trigger such an eruption. While imperfect, this model explains the observed crystallinity, the lack of andesite, phase chemistry and recent seismicity.

III. Depths ↓

Pressures were converted to depths using the model of Tassarra and Euchaurren (2012). Last mantle equilibration pressures calculated with Lee et al. (2009) gives results of 11-12kbar, which is the vicinity of the Moho interface depth. Pressures calculated from Cpx-Liq equilibrium (~3kar) that correspond to the main site of differentiation is estimated around 12km bsl.

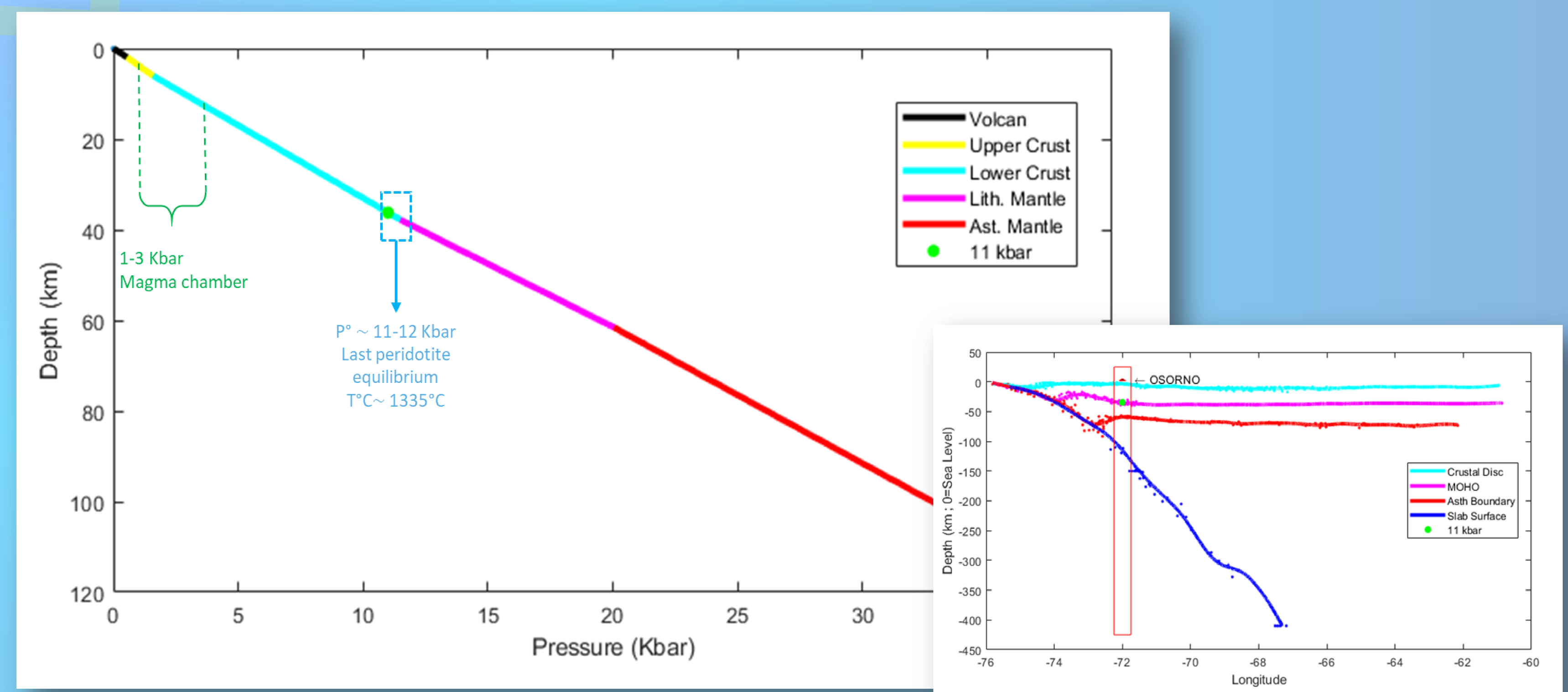

V. Recorded seismicity →

SERNAGEOMIN observatory reports each month major seismic events related to fracturation of brittle material below the volcano. We used these reports since 2015. The main part of the seismicity is located on the NW to the NNW flanks. It is interpreted here as recording lateral dyke propagation and sill emplacement at relatively shallow depth. Color and size of the dots are linked with the magnitude of the earthquake.

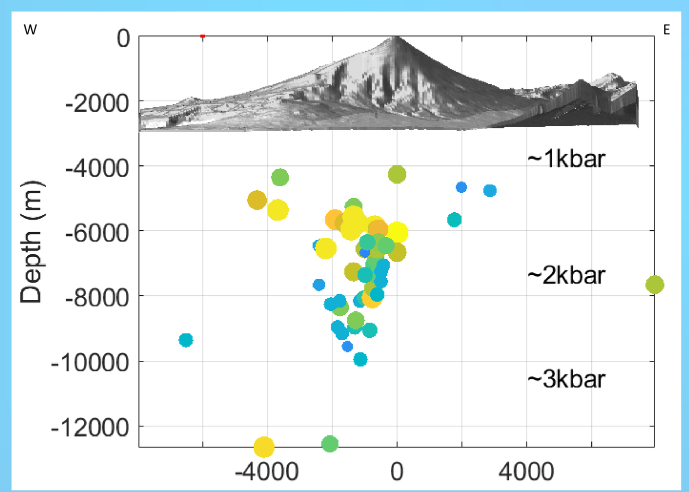

Conclusions:

The use of recent thermobarometric models revealed two main storage regions: (1) at the MOHO interface (1-1.2GPa) and (2), at the upper/lower crust interface with rather low pressures (likely ≤0.3 Gpa). While at (1) primary magmas differentiate, (2) is interpreted as the depth of major differentiation and volatile exsolution. Thermodynamic simulations (Gualda et al., 2012; Ghiorso & Gualda, 2015) support these (2) depth estimates and reproduce the main paragenesis by simple fractional crystallization at 0.1-0.2 GPa. Our results may explain the recent seismic unrest below Osorno (from 2015 to 2019) with earthquakes mostly taking place between 0.1-0.3 GPa (4-10km below the summit). We added our data to the recent geophysical model of the magmatic reservoir.

References:

Castro, J. M., Schipper, C. I., Mueller, S. P., Militzer, A. S., Amigo, A., Parejas, C. S. & Jacob, D. (2013). Storage and eruption of near-liquidus rhyolite magma at Cordón Caulle, Chile. *Bulletin of Volcanology* **75**, 702.

Coogan, L. A., Saunders, A. D. & Wilson, R. N. (2014). Aluminum-in-olivine thermometry of primitive basalts: Evidence of an anomalously hot mantle source for large igneous provinces. *Chemical Geology* **368**, 1–10.

Díaz, D., Zuñiga, F. & Castruccio, A. (2020). The interaction between active crustal faults and volcanism: A case study of the Liquiñe-Ofqui Fault Zone and Osorno volcano, Southern Andes, using magnetotellurics. *Journal of Volcanology and Geothermal Research* 106806.

Ghiorso, M. S. & Gualda, G. A. R. (2015). An H2O–CO2 mixed fluid saturation model compatible with rhyolite-MELTS. *Contributions to Mineralogy and Petrology* **169**, 53.

Gualda, G. A. R., Ghiorso, M. S., Lemons, R. V. & Carley, T. L. (2012). Rhyolite-MELTS: a Modified Calibration of MELTS Optimized for Silica-rich, Fluid-bearing Magmatic Systems. *Journal of Petrology* **53**, 875–890.

Harrison, T. M. & Watson, E. B. (1984). The behavior of apatite during crustal anatexis: Equilibrium and kinetic considerations. *Geochimica et Cosmochimica Acta* **48**, 1467–1477.

Lee, C.-T. A., Luffi, P., Plank, T., Dalton, H. & Leeman, W. P. (2009). Constraints on the depths and temperatures of basaltic magma generation on Earth and other terrestrial planets using new thermobarometers for mafic magmas. *Earth and Planetary Science Letters* **279**, 20–33.

McGee, L. *et al.* (2019). Stratigraphically controlled sampling captures the onset of highly fluid-fluxed melting at San Jorge volcano, Southern Volcanic Zone, Chile. *Contributions to Mineralogy and Petrology* **174**, 102.

Montalbano, S. PhD (2018). Processus de différenciation et sources des magmas du volcan Calbuco (CSVZ, Chili). University of Liège.

Moreno Roa, H., Lara, L. E. & Orozco, G. (2010). Geologia del volcan Osorno.

Morgado Bravo, E. E. (2019). Pre-eruptive conditions, crustal processes, and magmatic timescales recorded in products of Calbuco and Osorno volcanoes, Southern Andes. phd, University of Leeds.

Morgado, E., Morgan, D. J., Harvey, J., Parada, M.-Á., Castruccio, A., Brahm, R., Gutiérrez, F., Georgiev, B. & Hammond, S. J. (2019). Localised heating and intensive magmatic conditions prior to the 22–23 April 2015 Calbuco volcano eruption (Southern Chile). *Bulletin of Volcanology* **81**, 24.

Morgado, E., Parada, M. A., Contreras, C., Castruccio, A., Gutiérrez, F. & McGee, L. E. (2015). Contrasting records from mantle to surface of Holocene lavas of two nearby arc volcanic complexes: Caburgua-Huelemolle Small Eruptive Centers and Villarrica Volcano, Southern Chile. *Journal of Volcanology and Geothermal Research* **306**, 1–16.

Morgado, E., Parada, M. A., Morgan, D. J., Gutiérrez, F., Castruccio, A. & Contreras, C. (2017). Transient shallow reservoirs beneath small eruptive centres: Constraints from Mg-Fe interdiffusion in olivine. *Journal of Volcanology and Geothermal Research* **347**, 327–336.

Neave, D. A. & Putirka, K. D. (2017). A new clinopyroxene-liquid barometer, and implications for magma storage pressures under Icelandic rift zones. *American Mineralogist* **102**, 777–794.

Putirka, K. D. (2008). Thermometers and Barometers for Volcanic Systems. *Reviews in Mineralogy and Geochemistry* **69**, 61–120.

Rudnick, R. L. & Gao, S. (2003). Composition of the Continental Crust. *Treatise on Geochemistry* **3**, 659.

Ryan, W. B. F. *et al.* (2009). Global Multi-Resolution Topography synthesis. *Geochemistry, Geophysics, Geosystems* **10**.

SERNAGEOMIN activity reports since 2015 - http://sitiohistorico.sernageomin.cl/volcan.php?iId=35

Tassara, A. & Echaurren, A. (2012). Anatomy of the Andean subduction zone: three-dimensional density model upgraded and compared against global-scale models. *Geophysical Journal International* **189**, 161–168.

Vander Auwera, J., Namur, O., Dutrieux, A., Wilkinson, C. M., Ganerød, M., Coumont, V. & Bolle, O. (2019). Mantle Melting and Magmatic Processes Under La Picada Stratovolcano (CSVZ, Chile). *Journal of Petrology* **60**, 907–944.

Wan, Z., Coogan, L. A. & Canil, D. (2008). Experimental calibration of aluminum partitioning between olivine and spinel as a geothermometer. *American Mineralogist* **93**, 1142–1147.

Funded by a FNRS grant n° PDR T.0079.18

Corresponding author : tonin.bechon@uliege.be

EGU2020 poster n° : D1554 / EGU2020 – 4848